Biophotonics Congress:

Biomedical Optics Congress 2016 (Cancer/Translational/Brain/OTS)

Time-Resolved Reflectance Diffuse Optical Tomography with Silicon PhotoMultipliers

Judy Zouaoui[a], Lionel Hervé[a], Laura Di Sieno[b], Alberto Dalla Mora[b], Edoardo Martinenghi[b], Antonio Pifferi[b], Jacques Derouard[c] and Jean-Marc Dinten[a]

[a]*Univ. Grenoble Alpes, F-38000 Grenoble, France*
CEA, LETI, MINATEC Campus, F-38054 Grenoble, France
[b]*Politecnico di Milano, Dipartimento di Fisica, Piazza Leonardo da Vinci 32, Milano I-20133, Italy*
[c]*Univ. Grenoble Alpes, LIPhy, F-38000 Grenoble, France*
judy.zouaoui@cea.fr

Abstract: Time-resolved reflectance diffuse optical tomography on phantoms using Silicon photomultipliers (SiPMs) as detectors were carried out. We infer that SiPMs are promising new detectors to probe and accurately quantify biological tissues.
OCIS codes: (110.6960) Tomography; (100.6950) Tomographic image processing; (040.1880) Detection.

1. Introduction

The composition of turbid media such as biological tissues can be retrieved non-invasively using time-resolved (TR) diffuse optical tomography (DOT). This optical measurement is performed using a near-infrared pulsed laser source and time-resolved detection which provides the temporal distribution of photons arriving at the detector. In order to increase the sensitivity to the deep layers it is necessary to collect as many "late photons" as possible. Indeed, photons reemitted later are those that had higher chance to probe the medium in depth. New promising detectors, silicon photomultipliers (SiPMs) were recently introduced and studied in time-domain diffuse optics [1]. They permit to maximize light harvesting thanks to their wide active area of an array of hundred microcells composed of a single-photon avalanche diode (SPAD) [1-3]. In order to recover a 3D representation of biological tissues composition from a set of time-of-flight distributions recorded from a 2D horizontal scan of an optical probe at the medium surface, a 3D reconstruction algorithm is implemented following the signal processing of the data. In previous TR-DOT studies, the performances of SPAD have been evaluated and shown good detection in depth [4]. In this study, we evaluate the possibility to perform TR-DOT with SiPMs and demonstrate the performances of this device to accurately reconstruct the composition of turbid media. We present the first experimental results of TR-DOT achieved with SiPMs on phantoms composed of absorbing inclusions embedded in a turbid medium at different depths. The accuracy of localization and quantification are assessed.

2. Materials and Methods

To evaluate the potential of using SiPMs for TR-DOT, experiments in reflectance geometry were carried out on phantoms. The optical probe (Fig. 1(b)) consisted in a set of two optical fibers each connected to a SiPM detector (Part number C30742-11-050-T1, Excelitas Technologies, Canada) at a fixed distance of 30 mm from a third optical fiber connected to a near-infrared picosecond pulsed laser (Fianium, UK, 26 ps pulse width, 40 MHz repetition rate, λ = 820 nm). The SiPMs were coupled to two time-correlated single-photon counting boards synchronized with the laser pulses. SiPMs are driven by custom electronic circuits (designed at Politecnico di Milano) [2] in order to optimize their timing resolution. The phantom was composed of an absorbing inclusion moved at various depths from 5 to 30 mm in a background liquid phantom weakly absorbing and scattering based on a water dilution of India ink and Intralipid (reduced scattering coefficient μ_s' = 12 cm^{-1} and absorption coefficient μ_a = 0.07 cm^{-1}) (Fig. 1(b)). According to Martelli *et al.* [5] a totally black object can be used to mimic an absorbing inclusion of a given volume. Thus we decided to use a black PVC cylinder with 5 mm diameter and 100 mm^3 volume which, according to [5], is equivalent to an effective $\delta\mu_a$ of 0.15 cm^{-1} over a 1 cm^3 spherical volume. For each scan over the phantom, measurements were also done with the probe very far from the inclusion to acquire reference measurements.

The 3D maps of the absorption coefficient were obtained through a reconstruction algorithm based on a model where the propagation of light is governed by the diffusion equation, and where the information carried by the late photons is extracted using the Mellin-Laplace tranforms (MLT) of the TR measurements [6, 7]. Thanks to the combination of the perturbed and reference measurements detailed in [7] and the perturbation theory which gives us the variations of the Green's function (G) with variations of the absorption of the medium and the proprieties of the MLT [6] (p number of extracted transforms and n the index of the number of orders), we obtain the inverse system

to solve of the reconstruction algorithm. To have a computational system, the medium is spatial discretized on V_m (volume related node m) by the finite volume method (FVM). So, the final system to solve is the following:

$$Y_{sd}^{(p,n)(k)} = -\sum_{i+j+l=n} M_{sd,m}^{A(p,i)} . \sum_{m} G_{s,m}^{B(p,j)(k)} . \delta\mu_{a,m}^{(k)} . G_{d,m}^{B(p,l)(k)} . V_m \qquad (1)$$

with $Y_{sd}^{(p,n)(k)} = \sum_{e+f=n} M_{sd,m}^{B(p,e)} . G_{sd,m}^{A(p,f)} - M_{sd,m}^{A(p,e)} . G_{sd,m}^{B(p,f)(k)}$, the combination of the measurements M_{sd}^{A} and M_{sd}^{B} without (A) and with the inclusion (B) and the computed Green's functions of the direct model from the source indexed by s and the detector indexed by d. Thus the inverse problem reduces to the form $Y = WX$ where $X = \delta\mu_a$ is the absorption perturbation and W is the sensitivity matrix. The unknown X is determined using a conjugated gradient method that minimizes a generalized least squares criterion. Through an iterative process, $\delta\mu_a^{(k)}$ is updated in Eq.1 at each iteration k up to 10 and we finally obtain our reconstructed μ_a maps.

3. Results

In Fig. 1(a), the 3D reconstruction results of the totally black inclusion at the 6 different depths from 5 to 30 mm depth are shown. Results are represented in a vertical (z-y) and a horizontal (x-y) slices both passing through the expected center of the inclusion. The colorbar shows the quantitative scale of the reconstructed absorption coefficient distribution. The absorption perturbation appears as a spot surrounded by a more or less homogenous background whose μ_a is close to the expected value 0.07 cm^{-1}.

In the horizontal slide where we choose to do an asymmetric scan, the accuracy of the localization of the inclusion is 1 mm up to the 20 mm depth. By looking at the vertical slices, we see that the reconstructed inclusion moved in depth. The accuracy of the depth position of the inclusion in the vertical slice can be seen on Fig. 1(c) where the calculated centroid of the reconstructed perturbation is represented (red crosses) as a function of the expected depth (black). The reconstructed depth curve follows well the expected one within an accuracy of 3 mm up to 25 mm depth. However at 30 mm depth, we see a large underestimation of the depth position, in the 3D reconstruction we are no longer able to distinguish the inclusion and the colorbar scale does not raise from the background value.

About the quantification, the reconstructed absorption coefficient of the inclusion decreases with depth (see colorbars in Fig. 1(a)). Only at 10 mm depth is the reconstructed value in agreement with the expected value μ_a = 0.22 cm^{-1}. Additionally this study was part of a complete campaign where we probed a gradual range of 5 totally absorbing inclusions in order to evaluate the quantification performance and we demonstrate the ability to quantify up to an effective $\delta\mu_a$ equal to 0.4 cm^{-1} at 10 mm depth (results not shown).

4. Discussion and Conclusion

Our experimental results demonstrate the potential of SiPMs in TR-DOT to achieve an accurate localization of absorbing inclusions immersed in a turbid medium up to 25 mm depth. Puszka *et al.* [4] have already demonstrated that the accuracy of the localization of deep inclusions is improved when using fast-gated SPAD recently developed. Hopefully, in the future, also SiPM (composed of array of SPADs) could potentially be tailored for operation in time-gated mode and thus better results will be expected.

Concerning the quantitative determination of the absorption coefficient, some limitations are identified because we are able to have a good quantification only at 10 mm depth and up to $\delta\mu_a$ equal to 0.4 cm^{-1}. We observe a decrease of the quantification in function of the depth. To improve the accuracy of the quantification some modifications of the reconstruction algorithm could be investigated by regularization and working on new reconstruction approaches.

5. Acknowledgements

This work was performed within the framework of the LABEX PRIMES (ANR-11-LABX-0063) of Université de Lyon, within the program "Investissements d'Avenir" (ANR-11-IDEX-0007) operated by the French National Research Agency (ANR).

Funding from the EU project Laserlab-Europe (n. 654148) is gratefully acknowledged.

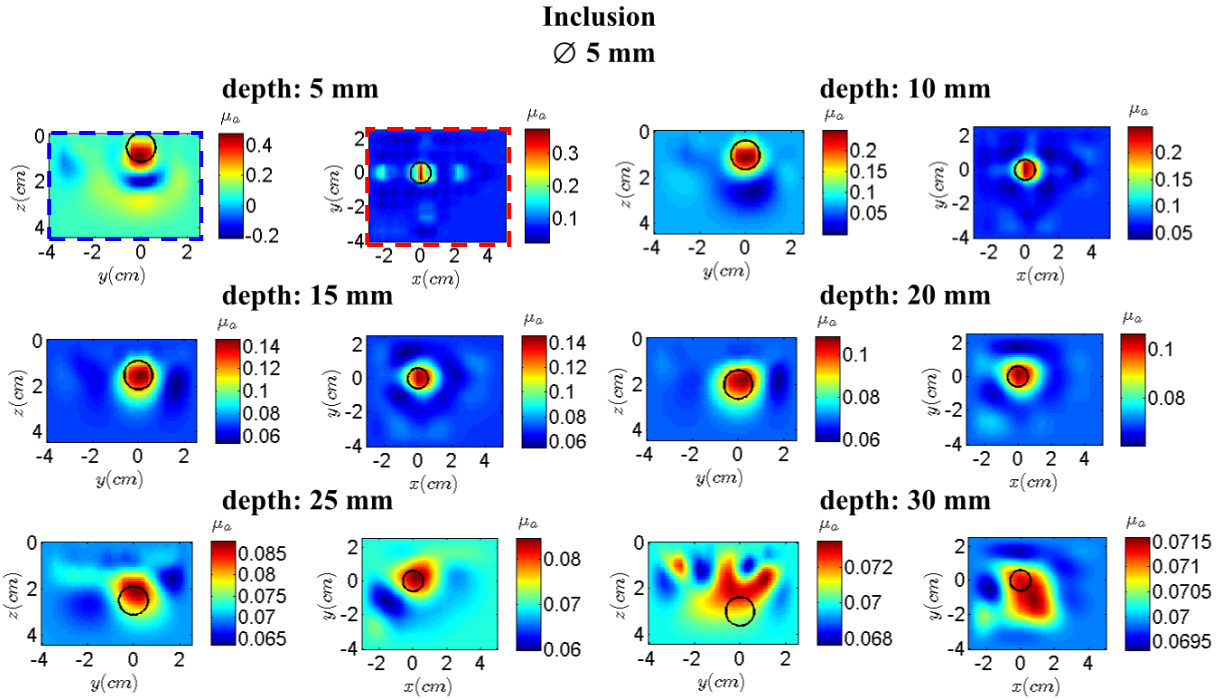

(a)

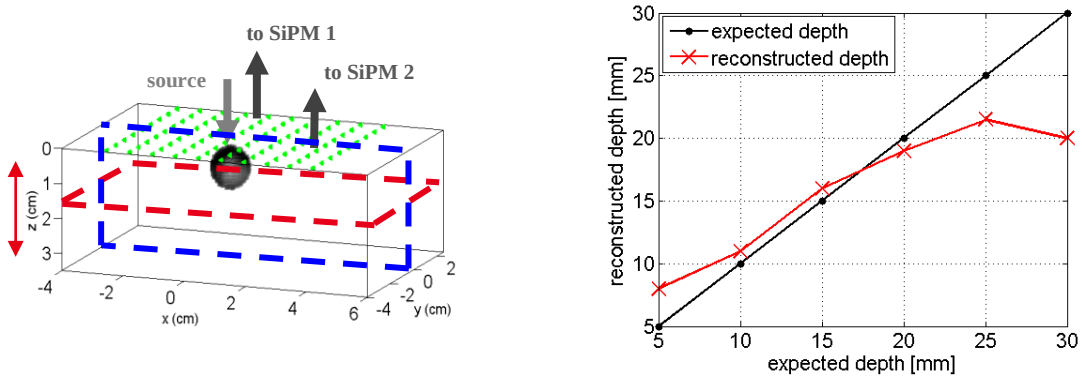

(b) (c)

Fig. 1. (a) 3D reconstructions in a vertical (x-z) and horizontal (x-y) slices passing through the center of a 5 mm diameter black PVC cylinder (100 mm^3 equivalent to $\delta\mu_a$ = 0.15 cm^{-1} over a 1 cm^3 volume [5]) at 5, 10, 15, 20, 25 and 30 mm depth. The black circle corresponds to a 1 cm^3 sphere and is centered on the expected position of the inclusion. (b) Schematic phantom with the totally black inclusion and source-detector probe with 30 mm source detector distance. (c) Reconstructed curve of the depth calculated by taking the centroid of a volume defined by the values above 50% of the difference between the maximum and background values. The black curve corresponds to the expected depths.

6. References

[1] A. Dalla Mora et al. "Towards next generation time-domain diffuse optics for extreme depth penetration and sensitivity," Biomed. Opt. Express, 6(5), 1749-1760 (2015).
[2] A. Dalla Mora et al. "Fast silicon photomultiplier improves signal harvesting and reduces complexity in time-domain diffuse optics," Biomed. Opt. Express, **23(11),** 13937-13946 (2015).
[3] E. Martinenghi et al. "Spectrally Resolved Single-Photon Timing of Silicon Photomultipliers for Time-Domain Diffuse Spectroscopy," IEEE Photonics Journal **7(4),** 1-12 (2015).
[4] A. Puszka, et al, "Time-resolved diffuse optical tomography using fast-gated single-photon avalanche diodes," Biomed. Opt. Express **4,** 1351-1365 (2013).
[5] F. Martelli et al. "Phantoms for diffuse optical imaging based on totally absorbing objects, part 2: experimental implementation," J. Biomed. Opt, **19(7),** 076011-076011 (2014).
[6] L. Hervé et al, "Time-domain diffuse optical tomography processing by using the Mellin–Laplace transform," Appl. Opt., **51,** 5978 (2012).
[7]A. Puszka et al. "Time-domain reflectance diffuse optical tomography with Mellin-Laplace transform for experimental detection and depth localization of a single absorbing inclusion," Biomed. Opt. Express, **4**, 569-583 (2013).